Available online at www.sciencedirect.com
ScienceDirect
Trans. Nonferrous Met. Soc. China 26(2016) 1843−1851
Transactions of Nonferrous Metals Society of China
www.tnmsc.cn

Diffusion bonding of Al 7075 and Mg AZ31 alloys: Process parameters, microstructural analysis and mechanical properties

Seyyed Salman SEYYED AFGHAHI[1], Mojtaba JAFARIAN[2], Moslem PAIDAR[3], Morteza JAFARIAN[2]

1. Department of Engineering, Faculty of Materials Science and Engineering, Imam Hossein University, Tehran 15816-18711, Iran;
2. Young Researchers and Elite Club, Science and Research Branch, Islamic Azad University, Tehran 14515775, Iran;
3. Department of Material Engineering, South Tehran Branch, Islamic Azad University, Tehran 1459853849, Iran

Received 7 August 2015; accepted 26 January 2016

Abstract: Al 7075 and Mg AZ31 alloys were joined by diffusion bonding method. Joining process was performed in pressure range of 10−35 MPa at temperatures of 430−450 °C for 60 min under a vacuum of 13.3 MPa. The microstructure evaluation, phase analysis and distribution of elements at the interface were done using scanning electron microscopy (SEM), energy-dispersive X-ray spectroscopy (EDS) and X-ray diffraction (XRD). The pressure of 25 MPa was determined as the optimum pressure in which the minimum amount of plastic deformation takes place at the joint. Different reaction layers containing intermetallic compounds, such as $Al_{12}Mg_{17}$, Al_3Mg_2 and α(Al) solid solution, were observed, in interfacial transition zone (ITZ). Thickness of layers was increased with increasing the operating temperature. According to the results, diffusion of aluminum atoms into magnesium alloy was more and the interface movement towards the Al alloy was observed. The maximum bond strength of 38 MPa was achieved at the temperature of 440 °C and pressure of 25 MPa. Fractography studies indicated that the brittle fracture originated from Al_3Mg_2 phase.
Key words: Al 7075 alloy; Mg AZ31 alloy; diffusion bonding; intermetallic compounds; interfacial transition zone; microstructure; mechanical properties

1 Introduction

Aluminum and its alloys are widely used in automotive, military and aerospace industries. They have high specific strength and corrosion resistance. On the other hand, magnesium alloys are the lightest structural alloys that are used in various industries [1−4]. Magnesium alloys have high specific strength and high damping capacity with easy recyclability. These properties have made magnesium alloys an ideal choice for diverse applications including portable electronic equipment and automotive parts [4]. According to the widespread use of these alloys in aerospace, automotive, electrical and chemical industries, in many cases the joining of Al and Mg is inevitable [5−7]. For example, a complex compound of Mg−Al was used in the engine and components of the space shuttles [8]. Joining of such dissimilar materials by conventional welding methods has become a challenge due to their diversities in physical properties such as melting temperature and thermal expansion coefficients. So, for bonding process of Al and Mg alloys, controlling of heating and melting, on both sides of the joint area, is critical [9]. Otherwise, the joining may lead to a weld zone without sufficient mechanical strength. In particular, the bonding of Al and Mg alloys is not possible by classical welding methods because of unexpected phase formation in the joint area. However, by the use of diffusion bonding methods, it is possible to join materials whose chemical and metallurgical properties are different [10]. In fact, diffusion bonding facilitates the joining of aforementioned materials. The quality of a joint is determined by its strength. To obtain the maximum strength, it is essential to control the relevant process parameters completely [11,12]. Among solid-state welding techniques for joining such alloys, the following processes could be cited: friction welding [13], explosive welding [14], transient liquid phase bonding [15] and diffusion bonding [16,17]. The formation of hard and brittle intermetallic compounds is a critical problem during the joining of Mg and Al. By using the vacuum

Corresponding author: Mojtaba JAFARIAN; Tel: +98-2332348850; E-mail: m.jafarian@iau-shahrood.ac.ir
DOI: 10.1016/S1003-6326(16)64295-4

diffusion bonding and controlling the time and temperature, the development of solidification cracks and high distortion stresses could be eliminated [18]. In this technique, parameters such as bonding temperature, pressure, holding time and surface roughness play an important role in determining the joint strength. For achieving the maximum strength, the formation and growth of intermetallic phases must be accurately controlled. A few literatures have focused on dissimilar joining of Mg and Al alloys via diffusion bonding [18−21]. LIU et al [18] developed the kinetic equations related to the growth of intermetallic phases for diffusion bonding of the Mg and Al 1060 alloys. MAHENDRAN et al [19] constructed the reference maps for selecting suitable parameters to achieve excellent quality bonds between Mg AZ31B and Al 2024 alloys [19]. JOSEPH-FERNANDUS et al [20] depicted the temperature–time and pressure–time diagrams for selecting appropriate parameters of Mg AZ80 and Al 6061 alloys diffusion bonding [20]. Furthermore, the maximization of strength in Al 6061 and Mg AZ31B diffusion joints was investigated by JOSEPH-FERNANDUS et al [21].

However, the diffusion bonding between Mg AZ31 and Al 7075 alloys is rarely addressed in the literature [22]. One of the most important challenges is achieving a joint with the maximum shear strength and the minimum deformation in base metals. Therefore, the aim of the present study is diffusion bonding of Mg AZ31 and Al 7075 alloys to achieve the optimum properties of the joint including the maximum bond strength and the minimum plastic deformation.

2 Experimental

The used materials for diffusion bonding were Al 7075 and Mg AZ31 alloys with corresponding chemical compositions that are summarized in Table 1.

Base metals with dimensions of 13 mm × 13 mm × 5 mm were cut from Mg AZ31 and Al 7075 slabs. Then,

Table 1 Chemical compositions of Mg AZ31 and Al 7075 alloys (mass fraction, %)

Alloy	Al	Mg	Si	Fe	Cr	Cu	Mn	Zn	Ti
Mg AZ31	3.17	Bal.	0.15	−	−	0.03	0.2	1.1	−
Al 7075	Bal.	2.6	0.12	0.45	0.2	1.5	0.15	5.6	0.03

the faying surfaces were polished by grinding to achieve the suitable quality for bonding process. Figure 1 illustrates the AFM micrographs of prepared samples. As observed, the average surface roughnesses for Al and Mg alloys decreased to 25.5 nm and 64.8 nm, respectively. Afterwards, the surfaces were ultrasonically cleaned in acetone bath for 15 min followed by subsequent drying. Diffusion bonding process was conducted at various pressures (10, 15, 20, 25, 30, 35 MPa) and temperatures (430, 440, 450 °C) for 60 min under the vacuum of 13.3 MPa. The heating rate was adjusted to 5 °C/min. To avoid any thermal shock, the samples were cooled down gently to the room temperature in the furnace. Figure 2 shows the apparatus which was used for the bonding process. Table 2 lists the process parameters for each sample.

The samples were sectioned perpendicularly to the bond line. Then, the resulting surfaces were prepared by grinding and polishing for microstructure and phase analyses. The microstructure of the joints was studied with scanning electron microscope (SEM). To determine the element distribution across the joint area, the elemental studies were done using an energy dispersive spectroscopy (EDS) detector that was attached to the SEM. The concentration profiles of the main elements were evaluated by linescan and elemental mapping. The micro-hardness tests were done at different points, in the joint regions using a 50 g Vickers micro-hardness tester.

To evaluate the mechanical properties of the joints, uniaxial tensile tests were conducted according to ASTM standard No. D1002−10. The fractured surfaces were studied using SEM. Finally, the phase constitution on the

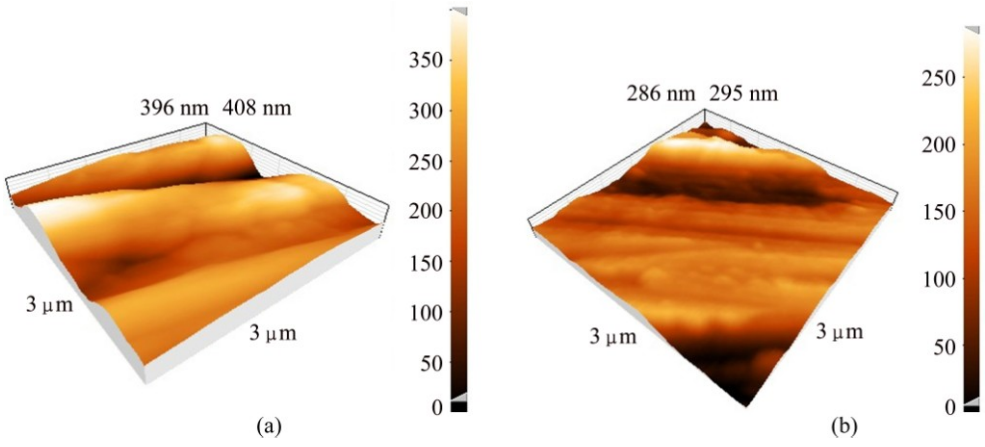

Fig. 1 AFM topography images of pre-bonding surfaces: (a) AZ31 Mg; (b) 7075 Al

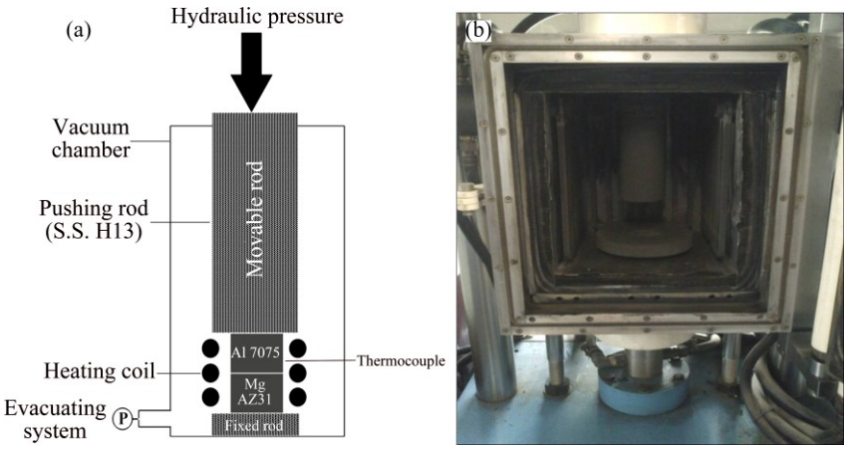

Fig. 2 Schematic diagram (a) and actual image (b) of bonding apparatus

Table 2 Samples bonded at different pressures and temperatures

Sample No.	Pressure/MPa	Temperature/°C
1	10	440
2	15	440
3	20	440
4	25	440
5	30	440
6	35	440
7	25	430
8	25	440
9	25	450

fractured surfaces was analyzed by means of X-ray diffraction (XRD).

3 Results and discussion

3.1 Determining optimum bonding conditions

Figure 3 shows the samples after the diffusion bonding under various pressures from 10 to 35 MPa at 440 °C for 60 min. The results showed that under pressures of 10, 15 and 20 MPa, the bonds were not strong enough and specimens were seperated by imposing a weak force. At lower bonding pressure, when surfaces are brought together, they contacted only at the limited protrusion points. Due to the slight contact regions, the strength of resulted joints was weak and so the surfaces deattached easily. Under the pressures of 30 and 35 MPa, an extreme deformation happened in Mg alloys, while under the pressure of 25 MPa the joints have the least amount of deformation. Figure 4 illustrates the obtained joints under pressure of 25 MPa at temperatures of 430, 440 and 450 °C for 60 min. As it can be seen, although the temperature increases from 430 to 450 °C, the Mg plastic deformation is negligible and its thickness decreases a little. Before the diffusion of atoms which is caused by temperature, the pressure led to the plastic deformation of surface and therefore the contact area increased by applying mechanical force. At first, voids were created through material protuberances and at surface contacts by mechanical pressure. After that, due to the lower strength of the Mg alloy than Al alloy, with increasing temperature, plastic deformation occurred on the rough surface of Mg via either conventional creep or super plasticity which led to filling of the voids [3,5]. During the bonding process, the mass transfer occurred along the curved surfaces to change the inequality condition to a stable state. The driving force of diffusion arises from the difference between surface free energies. Finally, by applying the pressure and temperature simultaneously, atomic motion accelerated and contact surface between two plates increased [3,5]. Following conclusions were obtained from the experimental observations on the basis of interface examinations.

1) When temperature of the bonding was lower than 430 °C (p=25 MPa and t=60 min), no bonding was achived between Al and Mg alloys due to insufficient temperature for atomic motion.

2) When the process temperature was greater than 450 °C (p=25 MPa and t=60 min), the bonding pressure automatically decreased after few minutes. This was due to the Mg alloy deformation at higher temperatures.

3) When pressure of the bonding was lower than 25 MPa (T=440 °C and t=60 min), no bonding occurred because of few contact points (between surface asperities).

4) When pressure of the bonding was greater than 25 MPa (T=440 °C and t=60 min), the plates were plastically deformed, leading to thickness reduction and outer edges bulging.

5) When the holding time was less than 60 min (p=25 MPa and T=440 °C), no bonding happened due to the insufficient time for atomic diffusion.

6) When the holding time was higher than 60 min

(p=25 MPa and T=440 °C), deformation of Mg alloy was observed.

3.2 Evolution of interfacial transition zone

Figure 5 shows the SEM−BSE images of joints heated at 430, 440 and 450 °C for 60 min. A full bonding has been created between two alloys due to the atomic interdiffusion. As it can be seen, joints do not have any defects such as impurities, micro-voids and incomplete fusion. There are three distinguishable layers between the two base alloys including Mg transition zone, middle diffusion zone and the Al transition zone which are totally called interfacial transition zone (ITZ). Figure 6 shows the effect of temperature on the thickness of ITZ. The average thickness of this zone increases with temperature from 17 to 30 μm (~76%). It is seen that the ITZ thickness chiefly depends on bonding temperature and therefore atomic diffusion. The formation of

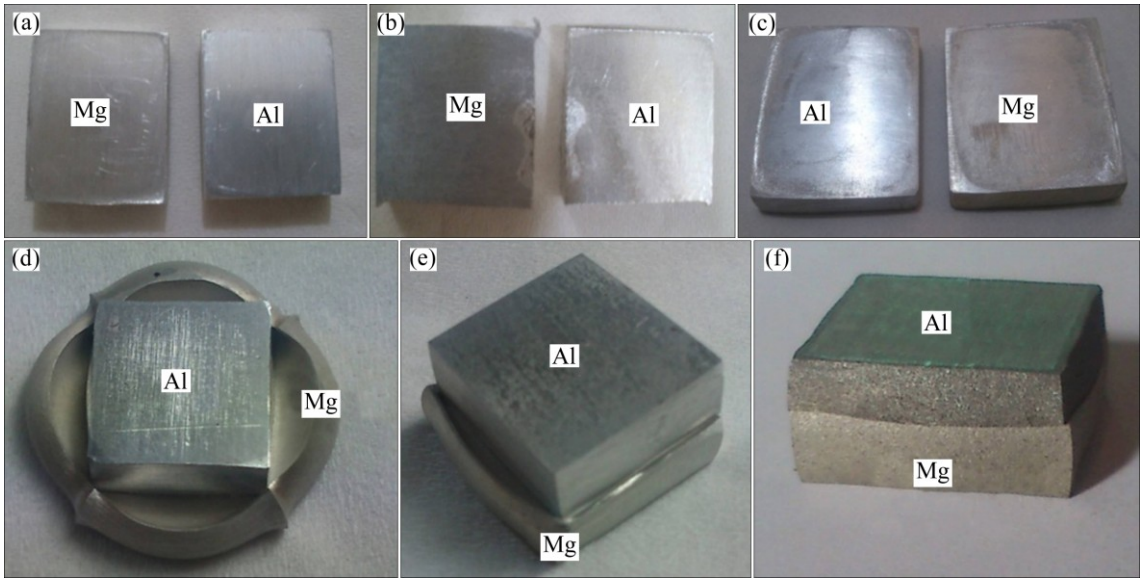

Fig. 3 Illustration of joints heated at 440 °C for 60 min under various pressures: (a) 10 MPa; (b) 15 MPa; (c) 20 MPa; (d) 25 MPa; (e) 30 MPa; (f) 35 MPa

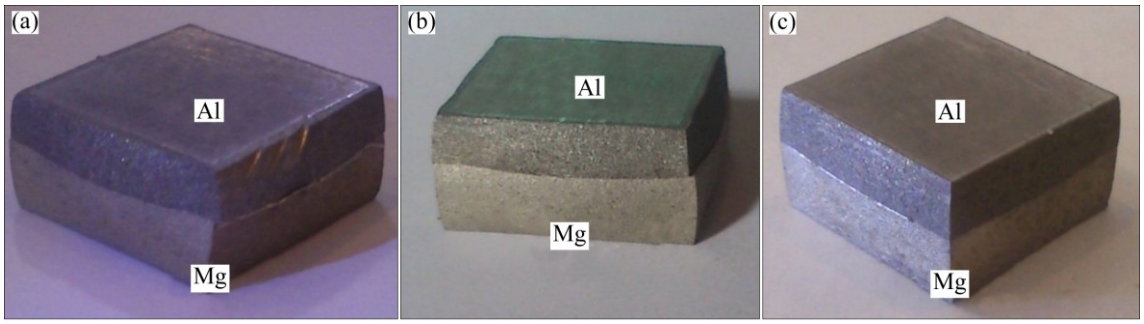

Fig. 4 Apparent features of Al/Mg alloys bonds heated at various temperatures: (a) 430 °C; (b) 440 °C; (c) 450 °C (t=60 min and p=25 MPa for all samples)

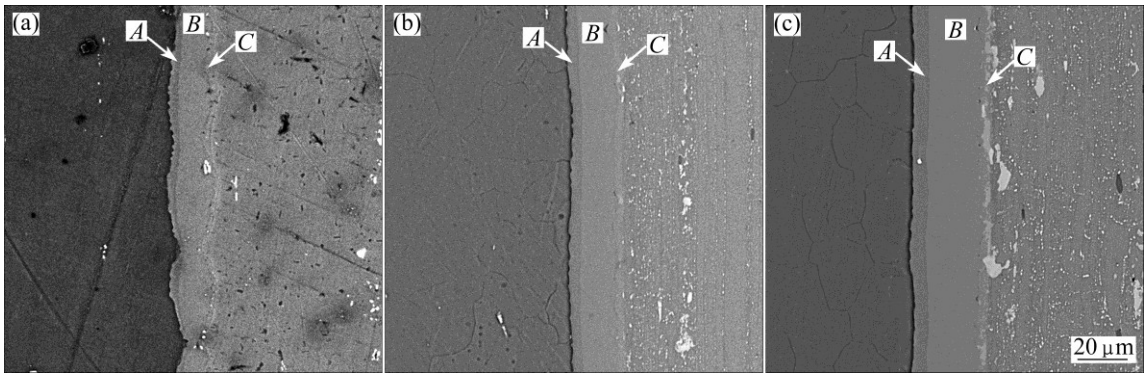

Fig. 5 SEM−BSE images of joints heated at 430 °C (a), 440 °C (b) and 450 °C (c)

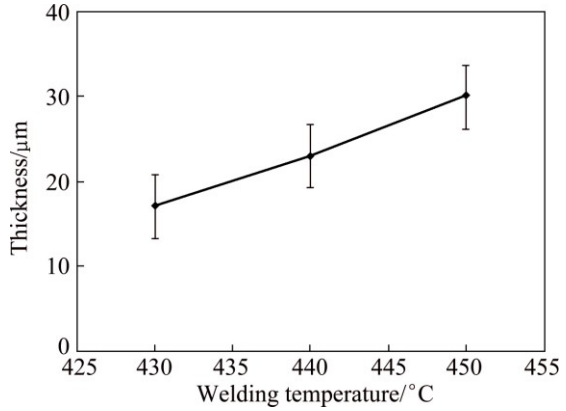

Fig. 6 Diffusion layer thickness as function of welding temperature (t=60 min)

intermetallic compounds at joint interface, that are marked by *A*, *B* and *C* in Fig. 5, has been determined by comparing the concentration of alloying elements through EDS analysis with the equilibrium phase diagrams [23] (Fig. 7). The obtained results are presented in Table 3.

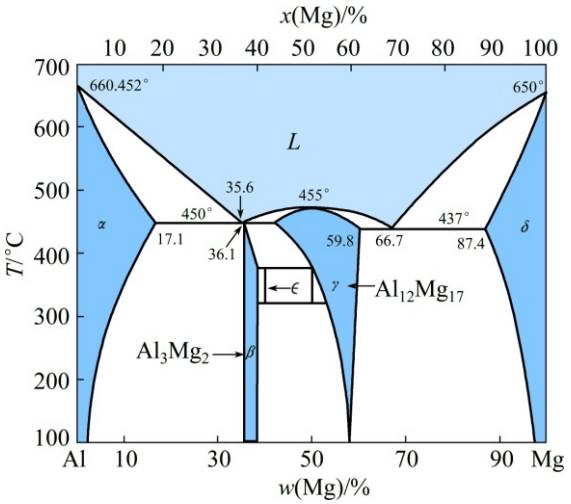

Fig. 7 Binary phase diagram of Al−Mg [21]

Table 3 EDS results of Regions *A*, *B* and *C* in Fig. 5

T/°C	Mass fraciton/%							
	A		*B*			*C*		
	Al	Mg	Al	Mg	Zn	Al	Mg	Zn
430	46.13	53.87	60.00	36.79	3.21	73.73	22.41	3.86
440	43.62	56.38	59.33	36.94	3.73	60.59	35.04	4.37
450	42.56	57.44	58.97	36.37	4.66	60.13	31.93	7.94

According to the Al−Mg binary phase diagram (Fig. 7), the existence of $Al_{12}Mg_{17}$ (γ), mixture of γ and β (Al_3Mg_2) and mixture of α(Al) solid solution and β are predicted in *A*, *B* and *C* layers, respectively. Assuming that the growth of each layer in ITZ, follows a parabolic kinetic process, the growth of layers can be expressed by the following equations [24−26]:

$$x \propto \sqrt{Dt} \tag{1}$$

$$D = D_0 \cdot \exp\left(\frac{-Q}{RT}\right) \tag{2}$$

where x is the thickness of reaction layers (m), t is the time of joining process (s), T is the joining temperature (K), D is the growth velocity of the reacting layer (m^2/s), D_0 is the growth constant (m^2/s), Q is the activation energy (kJ/mol) and R is the mole gas constant (8.314 J/(mol·K)). In this case, according to the ln X versus $1/T$ curve, the valuesof Q and D_0 could be calculated. Q and D_0 values of the reaction layers including *A*, *B* and *C* are given in Table 4.

Table 4 Q and D_0 values of reaction layers formed in ITZ

Region	Q/(kJ·mol^{-1})	D_0/(m^2·s^{-1})
A	87	5.3×10^{-2}
B	70	0.1
C	136	4.1×10^{-4}

As it can be seen, the growth rate of the Layer *B*, is more than that of other layers. The interdiffusion of Al and Mg elements, at 430, 440 and 450 °C for 60 min, is illustrated in Fig. 8, by line scan analysis (with length of 100 μm). The ITZ is the region at the both sides of the interface, where the concentration of solute atoms is over than 5% [24]. The size of this region can be determined from the concentration profiles. The result of line scan analysis at 430 °C indicates moderate diffusion across the interface (Fig. 8(a)). As temperature increases the concentration gradient reduces and the thickness of transition region increases. But in different situations, it was observed that the rate of diffusion of Al atoms into Mg alloy is more than that of Mg atoms into Al alloy. Since the atomic radius of Al (1/43 Å) is lower than that of Mg (1/6 Å), the mass fraction of Al in ITZ is more than that of Mg [16,17,19,20]. The activation energy for diffusion of smaller atoms is less and so, the smaller atoms have more diffusion rate. Therefore, the rate and the depth of diffusion for Al atoms are more than those of Mg atoms. The elemental map analysis was used to investigate the distribution of Al and Mg elements during diffusion bonding at different temperatures. Figure 9 indicates the elemental map of Mg and Al in the joints at various temperatures. Mg and Al elements are indicated by red and blue colors respectively. With increase of temperature, no change has happened in the initial position of Mg alloy, but the joint interface moves towards the Al alloy. Although the melting point of Mg alloy is less than Al alloy, but it is observed here that

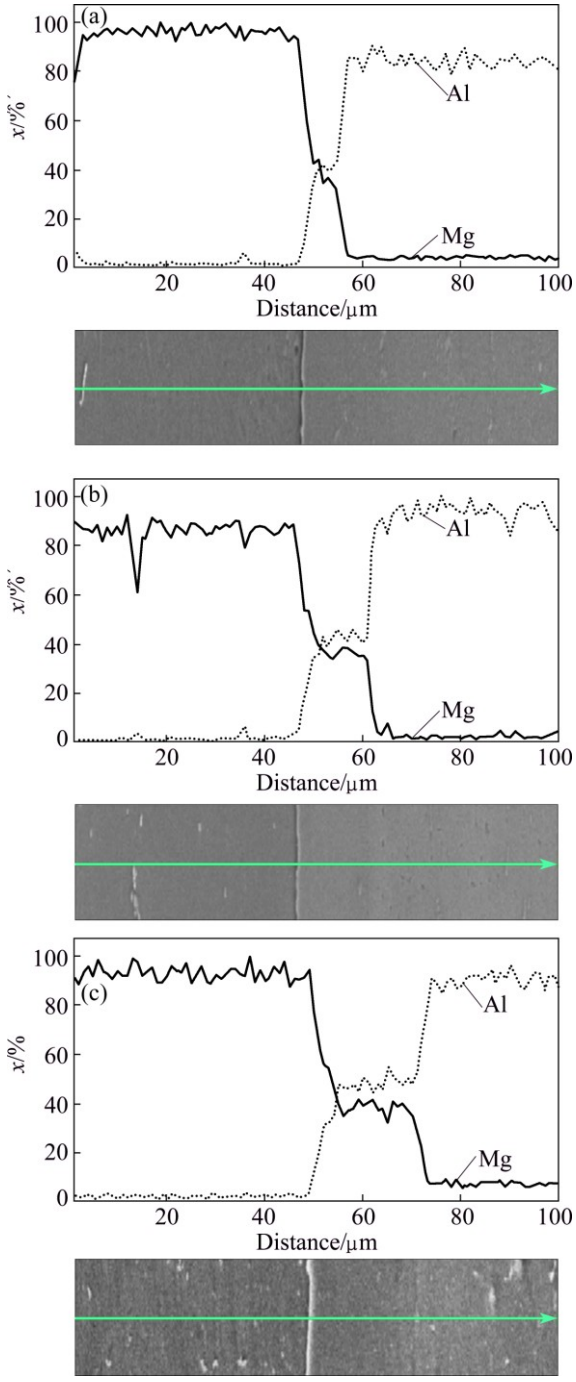

Fig. 8 Line scan analysis of joints at various temperatures of 430 °C (a), 440 °C (b) and 450 °C (c)

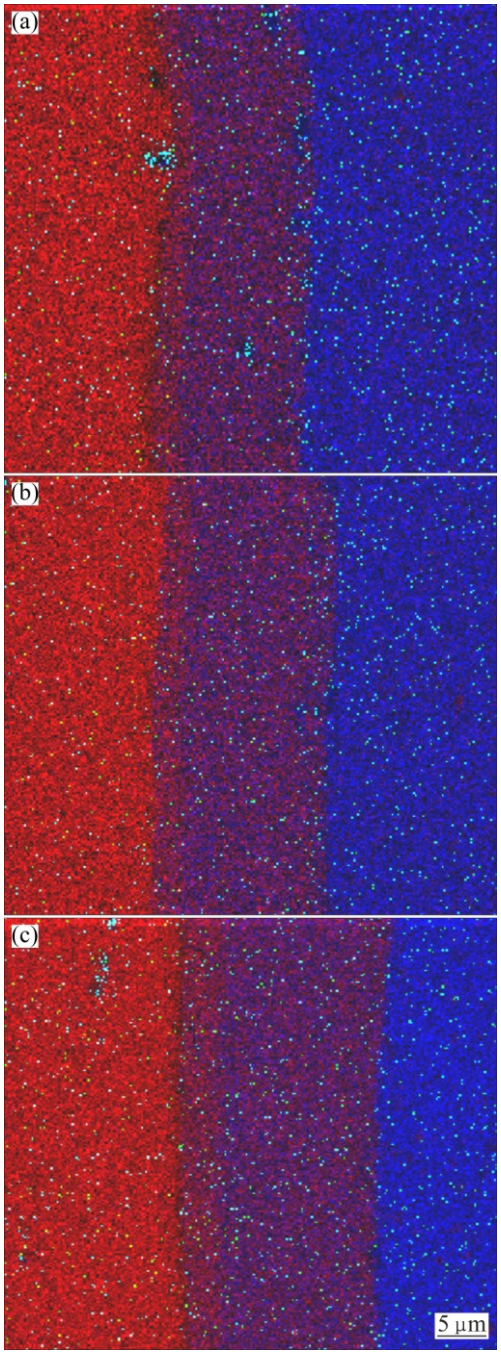

Fig. 9 Elemental map analysis of Mg and Al in joint area at temperatures of 430 °C (a), 440 °C (b) and 450 °C (c) (Red: Mg; Blue: Al)

with increase of temperature, the diffusion of Al atoms is greater than that of Mg. Furthermore, it is shown that at first, the interface line is rough but as the temperature increases, this line becomes smoother and diffusion of atoms gets more uniform. In Derby's theoretical model [27−30], possible diffusion bonding mechanisms were identified as: 1) plastic deformation of surface asperities; 2) power-law creep deformation of the surface; 3) diffusion of matter from interfacial void surfaces to growing necks, and 4) diffusion of matter from bonded regions at the interface to growing necks. According to the results, the formation process of different layers in the joint area could be predicted, as shown in Fig. 10.

1) Primarily, because of the concentration gradient, Al and Mg atoms of base metals diffuse into irregular interface with micro-voids. When their concentration reaches a critical value, a reaction occurs between Al and Mg elements and a layer containing Al−Mg will form (Fig. 10(a)).

2) Then, due to the greater diffusion of Al atoms into the Mg alloy, the aggregation of Al atoms, at the

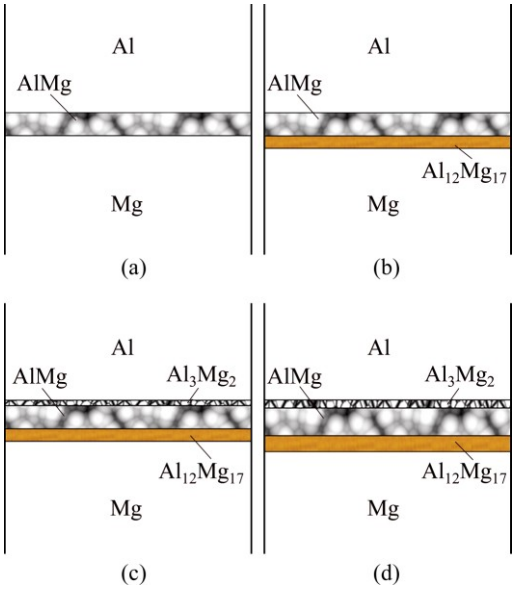

Fig. 10 Schematic illustration of diffusion bonding process of Al and Mg alloys: (a) First stage; (b) Second stage; (c) Third stage; (d) Fourth stage

interface layer and Mg region, will take place and the $Al_{12}Mg_{17}$ intermetallic compound would be formed (Fig. 10(b)).

3) At the same time, the diffusion of Mg atoms into Al alloy occurs and with increasing of Mg concentration at the interface and Al region, leading to formation of a layer containing Al_3Mg_2 phase (Fig. 10(c)).

4) Finally, according to the holding time, continuous diffusion of Al and Mg atoms occurs in ITZ, and the thickness of reaction layer increases with increasing time (Fig. 10(d)).

3.3 Evaluation of mechanical properties

The mechanical properties of the joints, are summarized in Table 5.

Table 5 Mechanical properties of joints at different temperatures

T/°C	Micro-hardness in ITZ (HV)	Shear strength/MPa
430	70	30
440	87	38
450	100	28

The results indicate that the value of microhardness is the highest in diffusion zone and changes uniformly across the joint area. The value of the microhardness in ITZ increases with increasing of bonding temperature. This fact is related to the formation and volume increment of intermetallic compounds. Moreover, according to the results, the maximum amount of shear strength (38 MPa) was obtained at 440 °C. Increase of temperature leads to an increase in the initial plastic deformation of surfaces by reducing the strength and causes the contact between faying surfaces. As a result, with increasing of deformation via creep process, enhancement of bond strength by displacement and removing of the primary interface, happen (440 °C). But, with further increasing of temperature, the volume of interfacial solid solutions and compounds, that are generally brittle intermetallic phases, increases and leads to reduction of the joint strength. In other work that was carried out on diffusion bonding of Al 6061 and Mg AZ31 alloys, higher values of shear strength than the peresent study, were obtained at lower temperature (430 °C), which is due to the lower thickness of ITZ [30].

Figure 11 shows the SEM images of the fracture surface of joints at 440 °C, after uniaxial tensile tests. Basically, due to the formation of intermetallic brittle compounds, ductility of bond area was lower than that of base metals. Figure 11(a) shows the image of fracture surface of Mg AZ31 sample. The river pattern can be seen clearly on the surface which shows the brittle and cleavage aspects of the fracture. In addition, the presence of micro-cracks is observable on the surface. According to the results of EDS analysis from specified points in Fig. 11(a), Point *A* contains 57.63% Mg (mole fraction) and 42.37% Al (mole fraction), which proves the presence of $Al_{12}Mg_{17}$ brittle phase, in this zone. Point *B* contains 40.93% Mg and 59.07% Al, which indicates the presence of Al_3Mg_2 phase. Precipitates at Point *C* contain 7.1% Mg, 71.15% Al, 5.89% Zn, 13.86% Fe, 0.66% Cu and 1.34% Cr. These Al-rich precipitates originate from

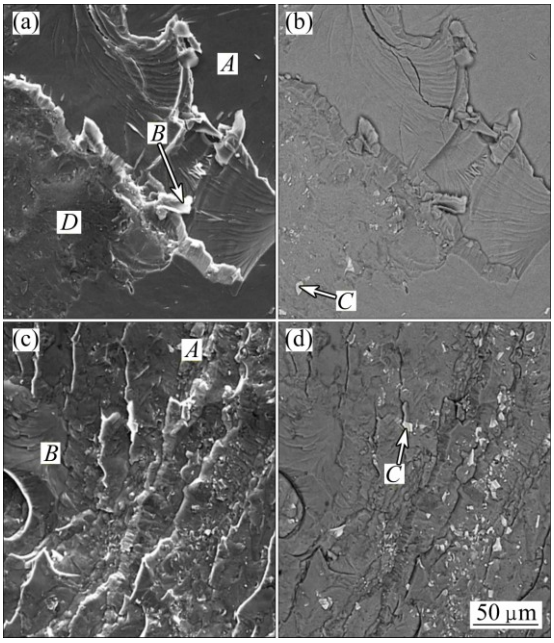

Fig. 11 SEM images of fracture surface: (a, b) Mg AZ31; (c, d) Al 7075

Al base alloy. The Area *D* containing 40.82% Mg and 59.18% Al which show the presence of Al_3Mg_2 brittle phase, is confirmed. This shows that the fracture has occurred between Al_3Mg_2 and $Al_{12}Mg_{17}$ layers. Figure 11(b) shows SEM images of fracture surface of the Al 7075 alloy. In this case, the river pattern is observable, which suggests also a brittle fracture. EDS analysis of marked points in Fig. 11(b), shows that Point *A* contains 40.9% Mg and 59.1% Al corresponding to Al_3Mg_2. Point *B* contains 58.21% Mg and 43.39% Al, which represents $Al_{12}Mg_{17}$ phase. Precipitates derived from Al alloy are also determined by Point *C* which contains 10.96% Mg, 27.96% Al, 3.75% Zn, 14.69% Fe, 0.5% Cu and 0.83% Cr. As it can be seen that, there are many micro-cracks on the fracture surface due to the presence of Al_3Mg_2, on the surface of Al alloy. This reflects that cracks have originated from this phase.

3.4 XRD studies

Figure 12 shows the XRD patterns of the joint at 440 °C after tensile tests from both sides of the fracture surface. According to the XRD results, the phases on the fracture surface of Al alloy, include Al_3Mg_2 and $Al_{12}Mg_{17}$ and the phases on the Mg fracture surface are $Al_{12}Mg_{17}$, Al_3Mg_2 and Mg. As it can be seen, at the temperature of 440 °C, a large amount of Al_3Mg_2 forms on the Al side.

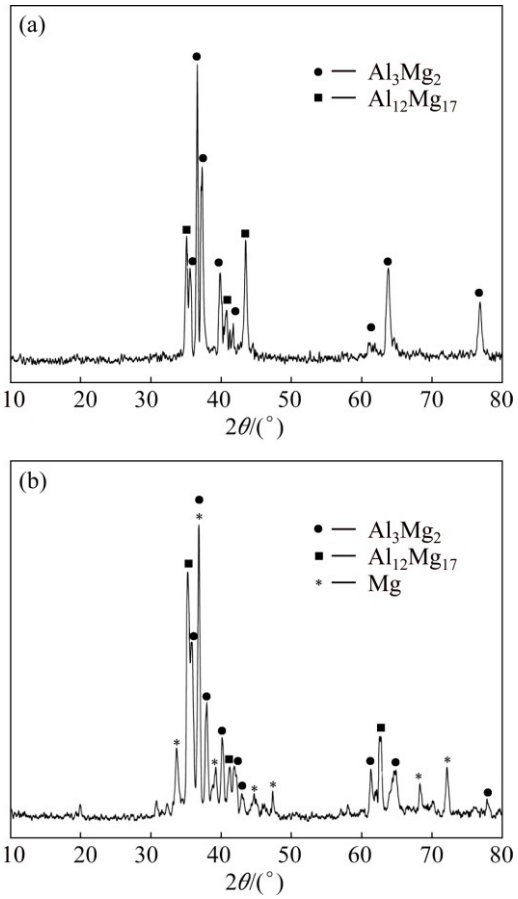

Fig. 12 XRD patterns of joint heated at 440 °C after tensile test: (a) Al side; (b) Mg side

4 Conclusions

1) At 440 °C, under uniaxial pressure of 25 MPa for 60 min, the deformation in the joint is the lowest among all samples and micro-voids were not observed at the interface.

2) The experimental results show that the α(Al) solid solution, $Al_{12}Mg_{17}$ and Al_3Mg_2 phases form at the diffusion interface. The distribution of these phases is less at lower processing temperatures and increases with process temperature due to the enhancement of interdiffusion coefficients.

3) According to experimental observations, a four-stage formation process for different layers at the joint area was proposed.

4) Optimum joining conditions achieved at 440 °C and 25 MPa exhibit the maximum shear strength of 38 MPa.

5) Fracture surface study indicates brittle and cleavage fracture type. The cracks initiate and propagate from Al_3Mg_2 brittle phase.

6) XRD results of fracture surfaces confirm the presence of the intermetallic phases such as Al_3Mg_2 and $Al_{12}Mg_{17}$ on the surface of Al and Mg.

Acknowledgement

The authors are grateful to Mahar Fan Abzar Co., Tehran, Iran for the facilities support.

References

[1] LI Y, LIU P, WANG J, MA H. XRD and SEM analysis near the diffusion bonding interface of Mg/Al dissimilar materials [J]. Vacuum, 2008, 82: 15−19.

[2] SONG G, AN G, LIU L M. Effect of gradient thermal distribution on butt joining of magnesium alloy to steel with Cu−Zn alloy interlayer by hybrid laser-tungsten inert gas welding. [J]. Materials and Design, 2012, 35: 323−329.

[3] DIETRICH D, NICKEL D, KRAUSE M, LAMPKE T, COLEMAN M P, RANDLE V. Formation of intermetallic phases in diffusion welded joints of aluminium and magnesium alloys [J]. Mater Sci, 2011, 46: 357−364.

[4] HARASH M, ATAYA S, ABDEL-HADY M A, EL-MAHALLAWY N. Microstructural characterization and kinetics of diffusion bonded AZ31/Al by hot press cladding [J]. Material Science and Technology, 2014, 45: 15−20.

[5] SEQUEIRA C A C, AAMAL L. Role of Kirkendall effect in diffusion processes in solids [J]. Transactions of Nonferrous Metals Society of China, 2014, 24(1): 1−11.

[6] SHANG Jing, WANG Ke-hong, ZHOU Qi, ZHANG De-ku, HUANG Jun, GE Jia-qi. Effect of joining temperature on microstructure and properties of diffusion bonded Mg/Al joints [J]. Transactions of Nonferrous Metals Society of China, 2012, 22(8): 1961−1966.

[7] ZURUZI A S, LI H, DONG G. Effects of surface roughness on the

diffusion bonding of Al alloy 6061 in air [J]. Materials Science and Engineering A, 1999, 270: 244−248.
[8] HUANG Y, RIDLEY N, HUMPHREYS F J, CUI J Z. Diffusion bonding of superplastic 7075 aluminium alloy [J]. Materials Science and Engineering A, 1999, 266: 295−302.
[9] KUNDU S, GHOSH M, LAIK A, BHANUMURTHY K, KALE G B, CHATTERJEE S. Diffusion bonding of commercially pure titanium to 304 stainless steel using copper interlayer [J]. Materials Science and Engineering A, 2005, 407:154−160.
[10] MA L, QIAO P, LONG W, HE D, LI X. Interface characteristics and mechanical properties of the induction brazed joint of magnesium alloy AZ31B with an Al-based filler metal [J]. Materials and Design, 2012, 37: 465−469.
[11] MIAO Y G, HAN D F, YAO J Z, LI F. Effect of laser offsets on joint performance of laser penetration brazing for magnesium alloy and steel [J]. Materials and Design, 2010, 31: 3121−3126.
[12] PENG L, YAJIANG L, HAORAN G, JUAN W. A study of phase constitution near the interface of Mg/Al vacuum diffusion bonding [J]. Materials Letters, 2005, 9: 2001−2005.
[13] CHOI D H, AHN B W, LEE C Y, YEON Y M, SONG K, JUNG S B. Formation of intermetallic compounds in Al and Mg alloy interface during friction stir spot welding [J]. Intermetallics, 2011, 19: 125−130.
[14] YAN Y B, ZHANG Z W, SHEN W, WANG J H, ZHANG L K, CHIN B A. Microstructure and properties of magnesium AZ31B−aluminum 7075 explosively welded composite plate [J]. Materials Science and Engineering A, 2010, 527: 2241−2245.
[15] LIU L M, TAN J H, ZHAO L M, LIU X J. The relationship between microstructure and properties of Mg/Al brazed joints using Zn filler metal [J]. Materials Characterization 2008, 59: 479−483.
[16] ZHAO L M, ZHANG Z D. Effect of Zn alloy interlayer on interface microstructure and strength of diffusion-bonded Mg−Al joints [J]. Scripta Materialia, 2008, 58: 283−286.
[17] WANG J, YAJIANG L, WANQUN H. Interface microstructure and diffusion kinetics in diffusion bonded Mg/Al joint [J]. React Kinet Catal Lett, 2008, 95: 71−79.
[18] LIU W, LONG L, MA Y, WU L. Microstructure evolution and mechanical properties of Mg/Al diffusion bonded joints [J]. Journal of Alloys and Compounds, 2015, 643: 34−39.
[19] MAHENDRAN G, BALASUBRAMANIAN V, SENTHILVELAN T. Developing diffusion bonding windows for joining AZ31B magnesium-AA2024 aluminium alloys [J] Materials and Design, 2009, 30: 1240−1244.
[20] JOSEPH-FERNANDUS M, SENTHILKUMAR T, BALASUBRAMANIAN V. Developing temperature-time and pressure-time diagrams for diffusion bonding AZ80 magnesium and AA6061 aluminium alloys [J]. Materials and Design, 2011, 32: 1651−1656.
[21] JOSEPH-FERNANDUS M, SENTHILKUMAR T, BALASUBRAMANIAN V, RAJAKUMAR S. Optimizing diffusion bonding parameters to maximize the strength of AA6061 aluminium and AZ31B magnesium alloy joints [J]. Materials and Design, 2012, 33: 31−41.
[22] CHEN Z T, LIN F, LI J, WANG F, MENG Q S. Diffusion bonding between AZ31 magnesium alloy and 7075 aluminum alloy [J]. Applied Mechanics and Materials, 2014, 618: 150−153.
[23] JIN Y J, KHAN T I. Effect of bonding time on microstructure and mechanical properties of transient liquid phase bonded magnesium AZ31 alloy [J]. Materials and Design, 2012, 38: 32−37.
[24] ZHANG J, SHEN Q, LUO G, LI M, ZHANG L. Microstructure and bonding strength of diffusion welding of Mo/Cu joints with Ni interlayer [J]. Materials and Design, 2012, 39: 81−86.
[25] AYDIN K, KAYA Y, KAHRAMAN N. Experimental study of diffusion welding/bonding of titanium to copper [J]. Materials and Design, 2012, 37: 356−368.
[26] TORUN O, KARABULUT A, BAKSAN B, CELIKYUREK I. Diffusion bonding of AZ91 using a silver interlayer [J]. Materials and Design, 2008, 29: 2043−2046.
[27] DERBY B, WALLACH E R. Theoretical model for diffusion bonding [J]. Metal Sci, 1982, 16: 49−56.
[28] DERBY B, WALLACH E R. Diffusion bonding: Development of theoretical model [J]. Metal Sci, 1984, 18: 427−431.
[29] ELZEY D M, WADLEY H N G. Modeling the densification of metal matrix composite monotape [J]. Acta Metall Mater, 1993, 41: 2297−2316.
[30] JAFARIAN M, KHODABANDEH A, MANAFI S. Evaluation of diffusion welding of 6061 aluminum and AZ31 magnesium alloys without using an interlayer [J]. Materials and Design, 2015, 65: 160−164.

Al 7075 和 Mg AZ31 合金扩散连接：工艺参数、显微组织分析和力学性能

Seyyed Salman SEYYED AFGHAHI[1], Mojtaba JAFARIAN[2], Moslem PAIDAR[3], Morteza JAFARIAN[2]

1. Department of Engineering, Faculty of Materials Science and Engineering, Imam Hossein University, Tehran 15816-18711, Iran;
2. Young Researchers and Elite Club, Science and Research Branch, Islamic Azad University, Tehran 14515775, Iran;
3. Department of Material Engineering, South Tehran Branch, Islamic Azad University, Tehran 1459853849, Iran

摘　要：采用扩散连接方法在压力范围 10~35 MPa、温度 430~450 °C、时间 60 min，真空 13.3 mPa 条件下连接 Al 7075 和 Mg AZ31 合金。采用扫描电子显微镜、X 射线能谱和 X 射线衍射分析合金的显微组织演变、相分析和元素分布。结果表明：25 MPa 为最佳的压力条件，在此条件下接头发生最小的塑性变形；在界面过渡区可观察到含不同金属间化合物如 $Al_{12}Mg_{17}$, Al_3Mg_2 和 α(Al)的固溶体反应层；随着温度的升高，反应层的厚度增大，更多的铝原子扩散进入镁合金，且界面朝着铝合金移动；在温度 440 °C、压力 25 MPa 下得到最大的结合强度 38 MPa。断口形貌研究表明，脆性断裂来自于 Al_3Mg_2 相。

关键词：Al 7075 合金；Mg AZ31 合金；扩散连接；金属间化合物；界面过渡区；显微组织；力学性能

(Edited by Xiang-qun LI)